J Eng Math (2007) 57:219–236
DOI 10.1007/s10665-006-9112-8

ORIGINAL PAPER

Global stability of the rotating-disk boundary layer

C. Davies · C. Thomas · P. W. Carpenter

Received: 12 June 2006/ Accepted: 24 October 2006 / Published online: 1 December 2006
© Springer Science+Business Media B.V. 2006

Abstract The global stability of the von Kármán boundary layer on the rotating disk is reviewed. For the genuine, radially inhomogeneous base flow, linearized numerical simulations indicate that convectively propagating forms of disturbance are predominant at all radii. The presence of absolute instability does not lead to the formation of any unstable linear global mode, even though the temporal growth rate of the absolute instability increases along the radial direction. Analogous behaviour can be found in the impulse solutions of a model amplitude equation, namely the linearized complex Ginzburg–Landau equation. These solutions show that, depending on the precise balance between spatial variations in the temporal growth rate and the corresponding shifts in the temporal frequency, globally stable behaviour can be obtained even in the presence of a strengthening absolute instability. The radial dependency of the absolute temporal frequency is sufficient to detune the disturbance oscillations at different radial positions, thus overcoming the radially increasing absolute growth, thereby giving rise to a stable global response. The origin of this form of behaviour can be traced to the fact that the cylindrical geometry of the rotating-disk flow dictates a choice of a globally valid time non-dimensionalization that, when properly employed, leads to a significant radial variation in the frequency for the absolute instability.

Keywords Absolute and convective stability · Cross-flow instability · Ginzburg–Landau equation · Global modes · Rotating disk

1 Introduction

The von Kármán [1] boundary-layer flow due to a rotating disk provides a model problem for the investigation of the instabilities of three-dimensional boundary layers and their role in the laminar-turbulent transition process. Because the flow has an inflection point, when resolved along a range of directions in the plane of disk, it is susceptible to the same type of inviscid crossflow instability that is present in swept-wing boundary layers.

C. Davies (✉) · C. Thomas
School of Mathematics, Cardiff University, Cardiff CF24 4AG, UK
e-mail: daviesc9@cardiff.ac.uk

P. W. Carpenter
School of Engineering, University of Warwick, Coventry CV4 7AL, UK

The rotating-disk configuration has the advantage that there is an exact similarity solution to the Navier–Stokes equations. The similarity structure is such that, in cylindrical co-ordinates aligned with the axes of rotation, all three velocity components of the flow have a profile across the boundary layer that is independent of the radius. But the actual magnitudes of the radial and the azimuthal components both increase in direct proportion to the radius. We shall see that this radial scaling of magnitudes has important consequences for the global stability of the flow.

Rather unusually for a wall-bounded external flow, and perhaps somewhat unexpectedly in view of the apparent completeness of earlier studies, it was found by Lingwood [2] that the von Kármán flow is absolutely unstable [3–5] at sufficiently large Reynolds numbers. She computed [2, 6] the critical Reynolds number for the onset of absolute instability to be $\mathrm{Re}_c = 507.3$, for a critical azimuthal wavenumber of approximately $n = 68$. The calculated value of Re_c is quite close to the Reynolds numbers at which the onset of the transition to turbulent flow has been observed in a number of different rotating-disk experiments, including Lingwood's own experimental study [7]. This, together with the relative constancy of the experimentally determined transition locations, has been interpreted to be strong evidence that the absolute instability has an important role in triggering transition.

1.1 Radial inhomogeneity and the parallel-flow approximation

Throughout Lingwood's investigation, a so-called parallel-flow approximation was applied, where the mean flow is simplified by taking it to be homogeneous along the radial direction. By selecting the mean flow at one given radial position and then artificially replicating this at all other radial locations, the parallel-flow approximation allows one to simplify the disturbance dependency along the radial direction to a normal-mode form. (The rotational symmetry of the mean flow, together with the inherent cylindrical geometry of the problem, ensures that the disturbance variation along the azimuthal direction can also be taken to have a normal-mode form.) The deployment of this approximated disturbance structure permits the derivation of a locally defined eigenvalue relation that is determined by the solutions of a set of ordinary differential equations. As is usual, these equations fix the wall-normal dependency of the disturbance across the boundary layer.

Without any homogenizing approximation, the linear stability problem necessarily involves a system of partial differential equations. These must be solved to determine the structure of the disturbance along the radial direction, as well as that along the wall-normal direction across the boundary layer. This additional complexity arises because of the radial dependency that appears in the similarity solution of the von Kármán flow. As was mentioned earlier, all the components of the mean flow keep the same normalized form of variation across the boundary layer, which means that the boundary-layer thickness remains constant. But the radial and azimuthal components are both scaled in magnitude in linear proportion with the radius. (This stems from the radially increasing tangential velocity of the disk surface, associated with the constant angular rotation rate.) Because the mean flow depends on the radius, the radial homogeneity of the linearized disturbance equations is destroyed, thus precluding the use of a normal-mode form for the radial variation of disturbances.

The question arises as to whether results obtained by applying a mean-flow radial homogenization do, in fact, provide a reliable guide as to what happens in the genuine inhomogeneous flow. Does the simplifying parallel-flow approximation, which amounts to the local removal of a characteristic feature of the rotating-disk flow, provide a good first step in the construction of solutions to the full problem? If so, the expectation would be that exact solutions of the locally approximate linear stability problem could be pieced together to obtain an approximate solution to the globally exact, linear stability problem. It would be usual to anticipate that any 'non-parallel' corrections, which might then be needed, would not give rise to significant qualitative alterations.

For the rotating-disk flow, we shall show that, though it is possible to assemble the local stability results to obtain some insight into the structure of solutions to the global stability problem, this assembly can lead to rather unexpected results. It turns out that important qualitative features of the behaviour found by using a locally based analysis are not preserved when the results of this analysis are pieced together to obtain a more global picture.

1.2 Recent physical experiments and numerical simulations

In addition to her theoretical analysis, Lingwood performed a careful physical experiment which appeared to provide strong evidence that absolute instability plays a key role in the transition to turbulence in the rotating-disk boundary layer. She traced the spatio-temporal evolution of impulsively generated disturbances and suggested that the trailing edge of these disturbances failed to propagate, in the commonly observed convective manner, beyond the radial location at which absolute instability was predicted to set in. The trailing edge appeared to asymptote to a constant radius, very close to that anticipated for the onset of absolute instability. However, Lingwood did not find any strong evidence in her experiment for a globally dominant frequency in the disturbance oscillations, which would have been expected if the absolute instability had given rise to an unstable linear global mode. (Note that, using the usual local non-dimensionalization that will be described later, one may set the Reynolds number equal to the non-dimensional radius, so that references to the Reynolds number and the radius can often be interchanged.)

For the genuine, radially inhomogeneous base flow, Davies and Carpenter [8] have carried out numerical simulations, conducted by solving the full linearized disturbance equations [9]. Investigations of the impulse response indicated that the absolute instability discovered by Lingwood does not in fact give rise to any unstable linear global mode. Except in artificially homogenized cases, the absolute instability was not found to lead to any sustained temporal disturbance growth, with a well-defined and globally constant frequency, at any of the radii that were considered. Instead, convective-type behaviour was found to dominate the flow for all of the Reynolds numbers investigated, even those taken well within the region of absolute instability.

There appears to be a *prima facie* disagreement between the numerical simulation results of Davies and Carpenter and the experimental evidence for an absolute instability that Lingwood had obtained by tracing the trailing-edge behaviour of wavepackets. This disparity can be explained, at least in part, by the difficulty of extrapolating the experimentally determined trailing edge as the disturbance grows and approaches radially outboard regions where nonlinear disturbances have already become significant. Moreover, in a physical experiment it can be very difficult to ensure that the controlled disturbance introduced into the flow remains linear at all desired locations. By contrast, nonlinear effects were deliberately excluded in the numerical simulations of Davies and Carpenter, by simply neglecting the appropriate terms in the governing equations, thus allowing the linear disturbance development to be investigated in a clear-cut manner at all radial locations.

A more recent physical experiment, conducted by Othman and Corke [10], but using disturbances with a much lower amplitude than was feasible for Lingwood, has provided convincing evidence that, in the linearized limit, convective instabilities are predominant. Othman and Corke found that, for an impulsively excited disturbance wavepacket, the trailing edge continues to move radially outwards with a finite convection velocity at all radii, including those that are located well within the absolutely unstable region. This and other aspects of their experimental results are in very good agreement with the behaviour predicted from the linearized numerical simulations conducted by Davies and Carpenter.

For higher-amplitude disturbances, Othman and Corke found behaviour that was more similar to that found in Lingwood's experiment. But there was again no evidence of any selection of a predominant global temporal frequency. They also attempted to make comparisons with the recent work of Pier [11], who has

demonstrated that a secondary form of absolute instability may develop on top of a finite-amplitude disturbance that has been generated by the primary absolute instability mechanism. This secondary absolute instability can only occur if the basic state has first been modified by a disturbance that has grown to a sufficiently large amplitude. Unfortunately, the comparison between Pier's predictions and the results of Othman and Corke's physical experiment was not very conclusive. In any case, as we shall see later, the primary absolute instability cannot necessarily be relied upon to provide a large enough disturbance for the secondary instability to take hold. For a linear disturbance developing in the genuine inhomogeneous flow, the temporal growth associated with the primary form of absolute instability turns out to be transient, for any given radial position.

1.3 Motivation for the present paper

The absence of any unstable linear global mode corresponding to the absolute instability is, at first sight, rather perplexing, because Lingwood's theoretical results indicate that the strength of the absolute instability increases in a marked fashion with the Reynolds number. Thus it would appear plausible that any stabilizing non-parallel effects which, if they exist, might be anticipated to become more and more weak as the Reynolds number is increased, would be unlikely to hold the absolute instability in check indefinitely.

Lingwood also performed an inviscid analysis that seemed to bolster the results obtained from her treatment of the viscous local eigenvalue problem. The inviscid analysis demonstrated that the absolute instability persisted in an appropriate inviscid limit. This suggests that the absolute instability should be robust even when it is embedded in the non-parallel flow, since non-parallel corrections ought to eventually become insignificant in the inviscid limit, at large enough radii.

However, there is a subtlety to the localized viscous stability analysis, as well as to its inviscid counterpart, that has often been overlooked. In the standard formulation, both the viscous and the inviscid treatment involve the use of a locally defined timescale for the non-dimensionalization of the time variation and the corresponding disturbance frequencies. The local timescale is constructed from the ratio between the constant boundary-layer thickness of the mean flow and the circumferential speed of the rotating-disk surface. The latter increases linearly with the radius. But there is also a global timescale, independent of the radius, that is defined by simply taking the inverse of the constant angular rotation rate of the disk. The fixed local frequency that characterizes the inviscid absolute instability actually corresponds, in the genuine radially inhomogeneous flow, to a collection of radially varying globally non-dimensionalized frequencies, with magnitudes that increase in linear proportion to the radius. It is thus not immediately obvious that the inviscid absolute instability can lead to the selection of any particular globally constant frequency for a globally unstable mode. Instead, a different frequency of oscillation might be anticipated for each distinct radial position. A similar reservation also applies when we consider the selection of the azimuthal mode number for the inviscid form of the absolute instability. (Some further discussion of the relationship between the azimuthal mode number used in the local stability analysis and its global counterpart will be included in the next section.)

The main aim of the present paper is to provide some further insight into why the rotating-disk flow can fail to give rise to any unstable linear global mode, even though, from the point of view of local stability analysis, it becomes increasingly absolutely unstable as the Reynolds number increases. An appreciation of why this can happen may be obtained by considering analogous behaviour in a mathematically much simpler system, namely the linearized complex Ginzburg–Landau equation. We will indicate how results determined from full numerical simulations for linearized disturbances in the rotating-disk flow may be modelled by, and systematically matched to, solutions of the Ginzburg–Landau equation.

2 An overview of numerical simulation results

In this section we provide a brief account of some of the numerical simulation results that were reported by Davies and Carpenter. Although we will also incorporate a few extensions to these simulations, the main focus will be on presenting results similar to those obtained previously, but in a manner that better serves our current purposes.

The numerical simulations were undertaken in order to investigate the spatio-temporal evolution of an impulsively generated linear disturbance wavepacket. The impulse was localized both in time and along the radial direction. For the azimuthal variation, a normal-mode form $\sim \exp(\mathrm{i}n\theta)$, with n an integer, could be assumed without any loss of generality. This is possible because there is an underlying azimuthal symmetry that is also reflected in the mean flow. Moreover, since linearity is imposed in the governing equations for the disturbance, there are no interactions between disturbances with different azimuthal mode numbers. (For more details, reference should be made to [8].)

Simulations could be conducted for either: (i) the genuine radially inhomogeneous flow, or; (ii) the artificially simplified homogeneous flow obtained by applying the parallel-flow approximation. Results for the latter case provided stringent validation for the numerical code. It was verified that, for the homogenized flow, impulsive excitation could trigger disturbances that grew continually in time, with growth rates and global temporal frequencies that were in excellent agreement with Lingwood's predictions for the absolute instability.

2.1 Mean flow and non-dimensionalization

Before proceeding any further, it may be helpful to review, in a little more detail, the form of the von Kármán mean flow, This will also facilitate a discussion of the possible choices for the non-dimensionalization.

In cylindrical co-ordinates $(r^*,\ \theta,\ z^*)$, defined in a rotating frame of reference that matches the motion of the disk surface, the dimensional mean flow can be written in the form

$$\mathbf{U}^*(r^*,\ z^*) = \left(U_r^*,\ U_\theta^*,\ U_z^*\right) = \left(r^*\Omega\, F(z),\ r^*\Omega\, G(z),\ \delta^*\Omega\, H(z)\right), \tag{1}$$

where Ω is the angular rotation rate of the disk, $\delta^* = (\nu/\Omega)^{1/2}$ is the boundary-layer thickness, with ν the kinematic viscosity, and $z = z^*/\delta^*$ is the non-dimensional wall-normal co-ordinate. (As usual, asterisks are used to denote dimensional quantities.) The three distinct functions F, G, H, which specify the von Kármán similarity solution, can all be determined from the solution of a coupled set of ordinary differential equations.

The constant boundary-layer thickness δ^* provides the reference length for the non-dimensionalization of distances, but there are two possible choices of reference scale for the velocity field. A locally based velocity scaling is obtained by using the circumferential disk velocity $r_l^*\Omega$ at some chosen dimensional reference radius r_l^*. This gives the mean flow in the non-dimensional form

$$\mathbf{U}_l(r,\ z) = \left(\frac{r}{\mathrm{Re}}F(z),\ \frac{r}{\mathrm{Re}}G(z),\ \frac{1}{\mathrm{Re}}H(z)\right), \tag{2}$$

where $r = r^*/\delta^*$ and $\mathrm{Re} = (r_l^*\Omega)\delta^*/\nu = r_l^*/\delta^* = r_l$ is the local Reynolds number, which is equal to the non-dimensional radius at the reference position. The globally defined velocity scale is given by $\delta^*\Omega$, which leads to an alternative non-dimensionalization of the mean flow as

$$\mathbf{U}_g(r,\ z) = \left(rF(z),\ rG(z),\ H(z)\right), \tag{3}$$

where the Reynolds number is, in effect, set equal to unity at all radial locations.

Using the local velocity scaling for the non-dimensionalization, we observe that the parallel-flow approximation amounts to the replacement of the co-ordinate r by the constant r_l in the linearized equations for

the disturbance evolution, whenever r makes an appearance in an explicit fashion, rather than just through the derivative $\partial/\partial r$. Thus, in all the terms that involve the mean flow, $\mathbf{U}_l(r, z)$ is replaced by $\mathbf{U}_l(r_l,\ z)$. A similar replacement simplifies the radial dependence of the Coriolis terms, as well as that of a number of other terms that arise because of the cylindrical geometry.

The local and globally defined choices of the velocity scale lead to local and global time non-dimensionalizations, in the manner described earlier. We can specify the local and global timescales to be $\delta^*/(r_l^*\Omega) = 1/r_l\Omega$ and $1/\Omega$, respectively. This means that the period for one rotation of the disk is equal to a constant $T_g = 2\pi$ time units when the global timescale is adopted, but increases with the Reynolds number in accordance with the relation $T_l = 2\pi$ Re when the local form of time dimensionalization is used instead. Thus if ω_l and ω_g represent, in turn, the local and global non-dimensional temporal frequencies corresponding to the same physical frequency, then we have the relation

$$\omega_g = \omega_l \mathrm{Re}. \tag{4}$$

In what follows we will drop suffixes denoting local and global time scaling, when referring to non-dimensional quantities. The appropriate non-dimensionalization should usually be clear from the context. Where it is not, the convention will be that complex frequencies ω are represented in terms of the locally scaled time, so that ω Re gives the corresponding global quantity.

For later reference, we note that a useful measure for assessing the time-dependent behaviour of a disturbance can be obtained by defining

$$\tilde{\omega}(r,t) = \frac{\mathrm{i}}{A}\frac{\partial A}{\partial t}, \tag{5}$$

where $A(r,t)$ is some specified measure of the complex disturbance amplitude. (Implicitly, we have taken the azimuthal variation to be of the normal-mode form noted previously. This ensures that the disturbance amplitude becomes complex-valued.) Provided that, in practice, the quantity $\tilde{\omega}$ is found not to vary too rapidly in either space or time, it can be interpreted as the complex frequency displayed by the disturbance at a particular radial position and instant of time. When analysing the numerical simulation data, we select the value of the azimuthal component of the perturbation vorticity at the rotating-disk surface so as to provide the most convenient measure for A, but other specifications for the disturbance amplitude do not alter the results significantly.

2.2 Numerical simulation results for the homogenized mean flow

As we have already noted, the behaviour observed in numerical simulations that were conducted using the parallel-flow approximation was found to be in very good agreement with the results of Lingwood's local stability analysis. When the Reynolds number Re and the azimuthal mode number n were selected so that absolute instability could be anticipated, impulsively excited forms of disturbance were seen to spread both radially inwards and outwards from the point where they were initiated. Given enough time, such disturbances propagate to reach any given radial position within the homogenized flow. At every radial point they eventually display oscillation frequencies and temporal growth rates that approach the values predicted from Lingwood's local stability analysis.

Figure 1 presents results for the large-time asymptotic temporal frequencies and growth rates determined from a series of different parallel-flow simulations that were conducted for a range of Reynolds numbers. The azimuthal mode number was kept constant in all of the simulations at the value $n = 68$, which is close to that for which Lingwood predicted absolute instability would first set in. The complex frequencies were calculated using the quantity $\tilde{\omega}$ that was defined by Eq. 5 in the previous section. Each plotted data point was obtained by estimating the limit

$$\omega = \lim_{t\to\infty} \tilde{\omega}(r_f, t), \tag{6}$$

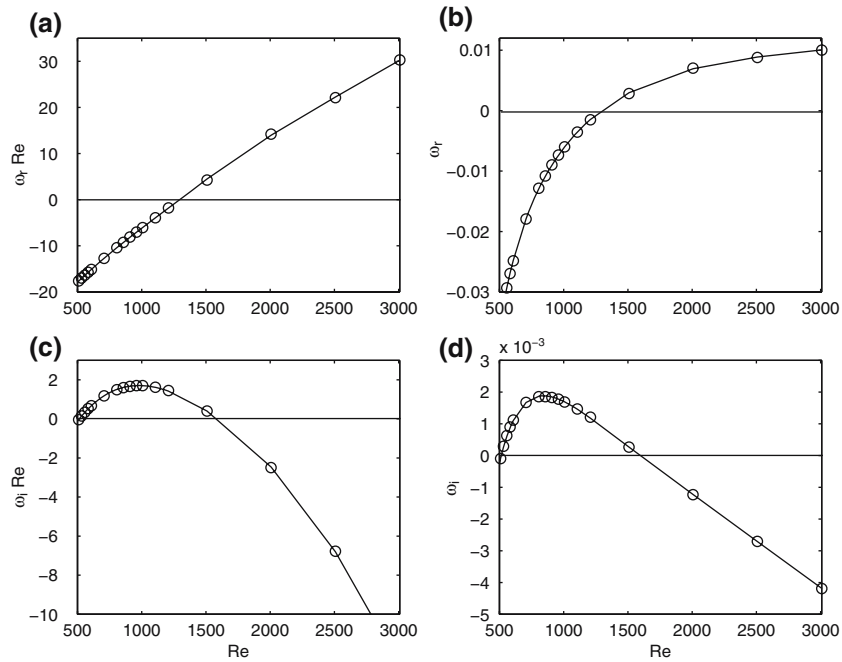

Fig. 1 Complex frequencies obtained in the large-time limit from simulations of impulsively excited disturbances in the homogenized flow at various Reynolds numbers Re. The azimuthal mode number is kept constant at $n = 68$. (**a**) ω_rRe; (**b**) ω_r; (**c**) ω_iRe; (**d**) ω_i. Each data point (○) corresponds to a result obtained from a separate numerical simulation conducted at the indicated Reynolds number

where r_f is the radial position at which the impulse was centred. The real part of ω thus represents the limiting value of temporal frequency, while its imaginary part gives the corresponding temporal growth rate. (It should be remarked that, within the context of parallel-flow simulations, the actual value of r_f holds no particular significance. Every radial position has the same stability properties, which is just another way of saying that the disturbance evolves in a radially homogeneous setting. But when making comparisons with non-parallel flow simulations, it is convenient to set $r_f = \mathrm{Re}$.)

The plots (b) and (d) included on the right-hand side of Fig. 1 show frequencies and growth rates that have been non-dimensionalized in the usual locally based manner. By contrast, the plots on the left-hand side, (a) and (c), show frequencies and growth rates that are non-dimensionalized using the global time-scale based on the disk-rotation period. The global form of non-dimensionalization must be utilized if the results obtained from different parallel-flow simulations are to be made commensurate. This is necessary when the local results are brought together in an attempt to understand the global stability of the genuine, radially inhomogeneous, flow.

It can be seen from the figure that there is a closed interval of Reynolds numbers for which the homogenized flow is absolutely unstable, for the chosen azimuthal mode number. This unstable range begins at a value $\mathrm{Re} \simeq 510$, which agrees with the result derived using a local stability eigenvalue analysis. It may also be noted that the absolute instability for $n = 68$ extends to Reynolds numbers that are very much larger (by a factor of about three) than those at which it has been possible to maintain a laminar flow in any of the rotating-disk experiments that have been conducted to date. The frequencies for the absolute instability can be seen to increase with the Reynolds number, with the locally non-dimensionalized frequencies asymptoting towards a constant. (This becomes more evident if simulation data points that were obtained for much larger Reynolds numbers than those shown in figure are also considered). Thus, the globally defined frequencies must eventually increase in direct proportion to the Reynolds number.

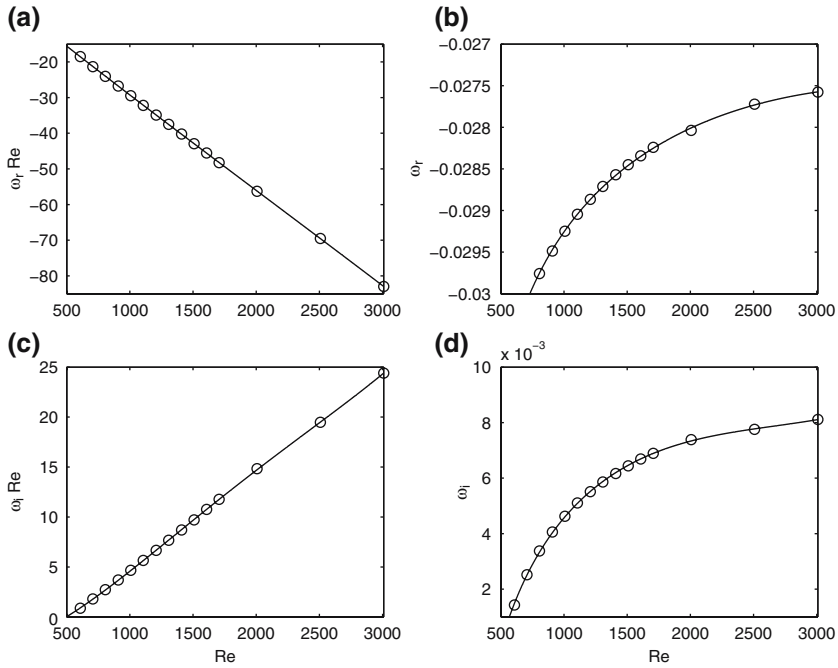

Fig. 2 Complex frequencies as in the previous figure, but in this case the azimuthal mode number is artificially varied so that at $\beta = n/\mathrm{Re} = 0.126$. (**a**) $\omega_r \mathrm{Re}$; (**b**) ω_r; (**c**) $\omega_i \mathrm{Re}$; (**d**) ω_i

It interesting to observe that the absolute unstable frequency passes through zero at $\mathrm{Re} \simeq 1,200$, which lies within the range of Reynolds numbers for which the $n = 68$ mode is unstable.

Figure 2 shows the asymptotic frequencies and growth rates obtained from another set of homogenized flow simulations. But this time the quantity $\beta = n/\mathrm{Re}$, rather than n, is held constant. The reason for imposing this rather artificial condition is that β is the azimuthal wavenumber that is treated most naturally within the local stability analysis. Strictly speaking it is unphysical to hold β constant, since n is constrained by the cylindrical geometry to take only integer values. Moreover, any linear disturbance in the radially inhomogeneous flow can be decomposed into independently evolving modes that each have a fixed value of n. Thus, in general, we should not anticipate that there would be any linear mechanism by which a disturbance could maintain a constant value of β in the genuine flow. But disregarding such difficulties of physical realization, the constant value $\beta = 0.126$ was selected in order to match the value predicted for the inviscid absolute stability by Lingwood. It can be seen that the frequencies and temporal growth rates, when represented using the locally based non-dimensionalization, appear to be approaching constant values as the Reynolds number increases. Unfortunately, it was not possible to extend this set of numerical simulations to very much higher Reynolds numbers, owing to convergence problems and the increasingly rapid growth of the disturbances. Nevertheless, the behaviour that could be discerned for the limited range of Reynolds numbers considered would seem to be compatible with the expectation that the complex frequency asymptotes to the inviscid absolutely frequency value $\omega = -0.0262 + 0.013$ obtained by Lingwood.

2.3 Simulation results for the radially inhomogeneous flow

As described in some detail by Davies and Carpenter [8], the behaviour of an impulsively excited linear disturbance turns out to be qualitatively different in the genuine inhomogeneous flow from that found in the homogenized flow.

When the homogenous flow is selected to be absolutely unstable, any disturbance to the flow displays continual temporal growth, with a growth rate that eventually approaches a constant value at all radial positions. The temporal frequency also asymptotes to a constant everywhere, though typically in a more rapid fashion than the growth rate. Such behaviour makes it possible to identify a unique complex frequency for the absolute instability at any given azimuthal mode number and Reynolds number. In fact, the well-defined nature of this complex frequency is implicit in the plots displayed in Figs. 1 and 2. Without it, the plots could not have been constructed.

By contrast, for the inhomogeneous flow, impulsively excited disturbances show no tendency to settle towards either a constant oscillation frequency or a constant temporal growth rate. This is illustrated by the time history plots in Figs. 3a, 4a, which were obtained from a numerical simulation for the inhomogeneous flow. (The construction of the related plots that are displayed in Figs. 3b, 4b, respectively, will be discussed later.) Both the radius r_f at which the impulsive excitation was applied, and the azimuthal mode number $n = 67$, were chosen to lie well within the absolutely unstable region of parameter space that is predicted for the radially homogenized version of the flow.

At the location of the impulsive forcing, the disturbance initially oscillates at a temporal frequency that is close to that which is found for a disturbance in the corresponding homogeneous flow with $\mathrm{Re} = r_f$. But, as Fig. 3a shows, the locally defined frequency at $r = r_f$ increases in a monotonic fashion with the passage of time. Because the frequency is negative this means that the disturbance oscillates more and more slowly. A similar form of local temporal frequency behaviour may be seen at the three other radial positions for which plots are displayed in the figure. After an initial transient interval, during which the frequency achieves a minimum, the same trend of increasing frequency is found. It may also be observed that, at any given later instant of time, the oscillation frequency at each radial position increases in an approximately linear manner with the radius. To some extent this spatial variation of the frequency is what might be expected. The numerical simulation results for the homogenized flow discussed earlier, in particular those presented for the asymptotic frequencies in Fig. 1a, indicate that the absolutely unstable frequency typically increases in an almost linear fashion with the Reynolds number. So since the Reynolds number used in each homogenized simulation corresponds to the non-dimensional radius in the genuine inhomogeneous flow, it might be anticipated that the oscillation frequency in the inhomogeneous flow would increase linearly with the radius. But a more elaborate explanation is called for in order to make sense of the variation of the locally defined frequencies over time. We will see later that further insight can be gained from comparisons with similar behaviour found in the impulse solutions of an appropriately selected linearized complex Ginzburg–Landau equation.

We now turn to the consideration of the locally defined temporal growth rates that were obtained from the numerical simulation of the inhomogeneous flow. These are displayed in Fig. 4a. It may be seen that, at all of the chosen radial positions, the growth rate eventually becomes negative, so the disturbance decays. This is clear at the impulse location and at the two selected positions nearest to this. For the most radially outboard position, the growth rate does not actually become negative during the displayed interval of time. But there is a very evident trend towards negative values. (As discussed in more detail in [8], it was not usually feasible to continue the numerical simulations to arbitrarily large times. This was mainly because of the difficulties in capturing the enormous growth of the wavepacket maximum, as it propagated radially outwards away from the excitation radius.)

The disturbance decays at all times at the selected radial position which is inboard from the impulse location. At the impulse location itself, there is a brief period during which the disturbance grows, but this is not sustained. At the two positions radially outboard from the impulse radius, there is a longer period of growth. The length of time over which the disturbance grows increases with the radius, though part of this growth is associated with the fact that the disturbance needs to propagate from the impulse location to the outboard radial positions. There is also some suggestion that, at large enough times, the locally defined growth rate, for any given time instant, increases linearly with the radius. As for the locally

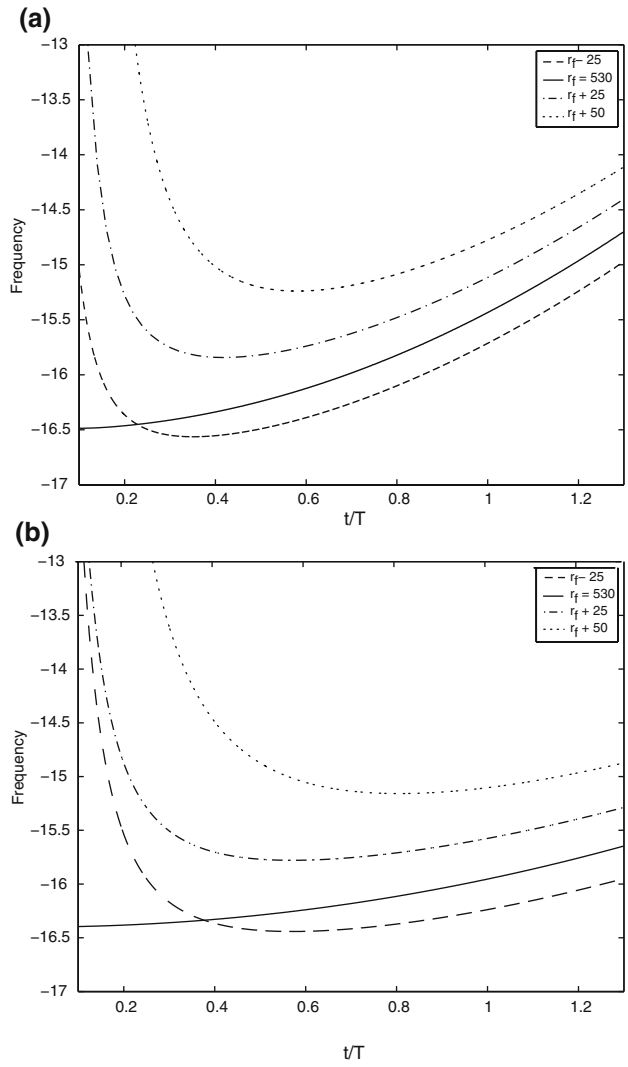

Fig. 3 Evolution of locally defined temporal frequencies for an impulsively excited disturbance in the inhomogeneous flow. Plots are shown for four equally spaced radii that include the location where the impulse was centred $r = r_f = 530$, one radially inboard location $r = r_f - 25$ and two radially outboard locations $r = r_f + 25$, $r = r_f + 50$. The azimuthal mode number is $n = 67$. (**a**) Results determined from a direct numerical simulation. These were obtained by calculating the real part of the complex frequency $\tilde{\omega}(r,t)$ defined by Eq. 5. (The disturbance amplitude was measured from the azimuthal component of the disturbance vorticity at the disk surface.); (**b**) Corresponding results constructed using a Green's function solution of the linearized complex Ginzburg–Landau equation with a linearly varying complex growth parameter $\mu = \mu_0 + \mu_1(r - r_f)$ (The frequencies and time are both non-dimensionalized using the global timescale.)

defined temporal frequencies, this linear dependency is likely to be associated with the corresponding variation in the growth rates with the Reynolds number for the homogenized flow. But, with the exception of the most radially inboard position plotted in the figure, the growth rates for the homogeneous flow, at Reynolds numbers matching the selected radii, would all asymptote to positive values. Some further explanation is thus needed as to why the disturbance decays in the inhomogeneous flow, even though it reaches more and more absolutely unstable locations as it spreads radially outwards from its source.

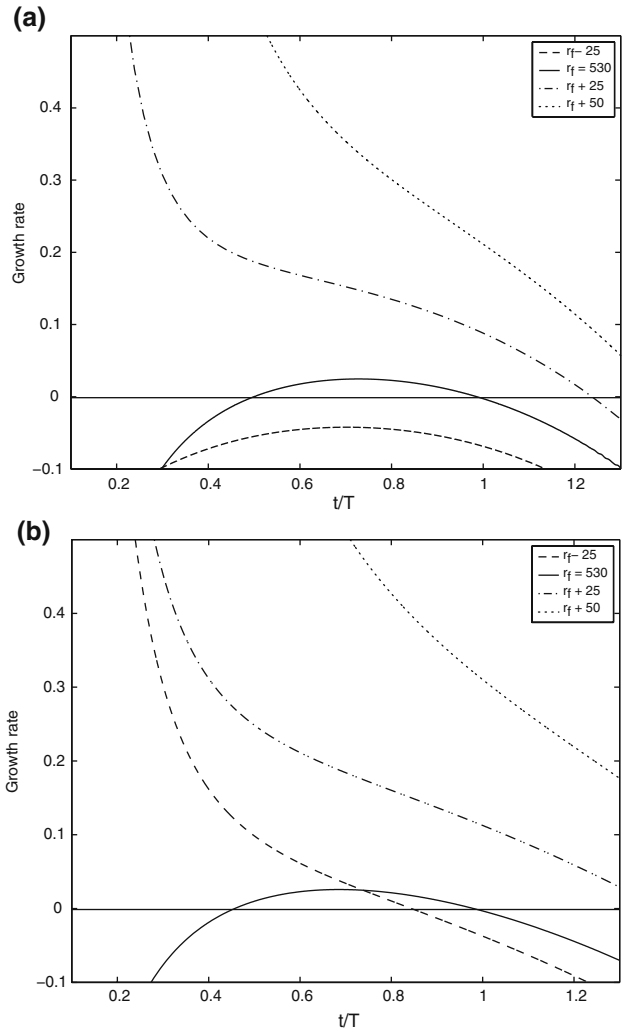

Fig. 4 Evolution of locally defined temporal growth rates for an impulsively excited disturbance in the inhomogeneous flow. Plots are shown for four equally spaced radii, as in the previous figure. The azimuthal mode number is $n = 67$ and the forcing is centred at $r_f = 530$. (**a**) Results determined from a direct numerical simulation. These were obtained by calculating the imaginary part of the complex frequency $\tilde{\omega}(r,t)$ defined by Eq. 5; (**b**) Corresponding results constructed using a Green's function solution of the linearized complex Ginzburg–Landau equation with a linearly varying complex growth parameter $\mu = \mu_0 + \mu_1(r - r_f)$ (The growth rates and time are both non-dimensionalized using the global timescale.)

3 Modelling using the linearized Ginzburg–Landau equation

We shall now describe how the absence of any unstable linear global mode, in the genuine radially inhomogeneous rotating-disk flow, can be explained by considering analogous behaviour in the solutions of the linearized complex Ginzburg–Landau equation.

The nonlinear version of the complex Ginzburg–Landau equation arises in a very wide variety of different contexts [12]. But for present purposes we only need the equation in its linearized form, which provides a simple and convenient model for analyzing the linear space-time development of a disturbance amplitude $A(r,t)$. It can then be written as

$$\frac{\partial A}{\partial t} + U\frac{\partial A}{\partial r} = \mu A + \gamma \frac{\partial^2 A}{\partial r^2}. \tag{7}$$

The terms multiplied by U, μ and γ represent, respectively, the effects of: (i) disturbance convection; (ii) linear temporal growth and temporal oscillation (the latter is only included in an explicit manner if μ is taken to be complex); (iii) diffusion and dispersion. In the case where all three of the quantities U, μ and γ are taken to be independent of the spatial co-ordinate r, the linearized complex Ginzburg–Landau equation can be thought of as modelling the development of a disturbance in a spatially homogeneous flow, since every spatial position r is fully equivalent to all others. This spatial homogeniety is destroyed if any one of U, μ and γ is allowed to vary with r. It is then possible to associate the Ginzburg–Landau equation with a spatially inhomogeneous flow.

In what follows we will refer to the real part of μ, evaluated at a particular value of r, as being the local temporal growth rate and call its imaginary part the local temporal frequency. But it should be kept in mind that this terminology can be slightly misleading. For example, it is simple to show that if U, μ and γ are all constant, then $\mathfrak{Re}(\mu) - \mathfrak{Re}(U^2/(4\gamma))$, rather than $\mathfrak{Re}(\mu)$, gives the long-term growth rate for solutions triggered by an impulsive excitation. (The relevant Green's function solution will be stated later.) Moreover, any constant-frequency component of the solution can always be effectively reset to a zero frequency, by means of a simple transformation. This is possible because it is usual to interpret any complex amplitude solution $A(r,t)$ of the Ginzburg–Landau equation to be the envelope of some wavepacket or wavetrain, with an underlying space–time variation of the normal-mode form $\exp \mathrm{i}(\alpha r - \omega t)$. In the most general case, the normal-mode spatial wavenumber α and temporal frequency ω may both be allowed to be complex, but they are more usually taken to be real. If the normal-mode component is incorporated then the 'full' disturbance has the structure $A(r,t)\exp \mathrm{i}(\alpha r - \omega t)$. The inherent ambiguity of this factored decomposition means that it is always possible to assume, without any loss of generality, that the multiplier μ is purely real, whenever it is also constant. Any purely harmonic time oscillations included within $A(r,t)$ can simply be factored out into the normal-mode part of the disturbance variation. However, if μ is spatially dependent, then it cannot be reset to be real, unless it happens to have a constant imaginary part. This would give an unnecessary restriction to cases where just the growth rates, but not the temporal frequencies, were allowed to be spatially varying.

By introducing a spatial dependence into μ, while retaining constant values for U and γ, we can build a simple, yet instructive, model for a disturbance wavepacket developing in an inhomogeneous flow with spatially dependent stability properties. As should be clear from the discussion in the previous sections of this paper, radially dependent absolute-instability frequencies are a key feature of the rotating-disk boundary layer, as are radially dependent temporal growth rates. So some measure of variation in the imaginary part of μ, as well as in its real part, must be incorporated if there is to be any prospect of correctly capturing the effects due to the radial changes in the local stability of the rotating-disk flow.

We shall see that by simply prescribing a linear variation $\mu = \mu_0 + \mu_1(r - r_f)$, where r_f is some reference position and μ_1 is complex, we can construct solutions of the linearized complex Ginzburg–Landau equation that are in very good agreement with the numerical simulation results. This is notwithstanding the fact that we have not made any systematic attempt to derive the Ginzburg–Landau equation from the far more complicated system of partial differential equations that governs the development of linearized disturbances in the rotating-disk flow. Although such a derivation is possible for the more simple case of a slowly spatially developing shear flow [4], there have been some studies which suggest that the derivation cannot be readily carried over to the case of cross-flow vortices in three-dimensional flows. Gajjar [13] and Gajjar et al. [14] derived a novel integro-partial differential equation, rather than a nonlinear Ginzburg–Landau equation, when they deployed a very plausible set of asymptotic scalings to study the nonlinear development of disturbances in three-dimensional boundary layers such as the rotating-disk flow. Interestingly, the linearized version of their new disturbance amplitude equation does not retain any diffusion term that involves second-order spatial derivatives. But we shall see that the inclusion of a diffusion term seems to be crucial to the successful modelling of the behaviour found in our numerical simulations.

3.1 Impulse solutions of the linearized Ginzburg–Landau equation

Hunt and Crighton [15, 16] obtained analytic solutions of the linearized complex Ginzburg–Landau equation for cases where the multipliers U and μ were given a prescribed linear or quadratic dependence on the spatial co-ordinate r. They determined the Green's function $G(r,t)$ representing the response to an impulsive forcing of the form $\delta(r)\delta(t)$, applied to the right-hand side of Eq. 7. As usual, δ denotes the Dirac delta function. In order to simplify the notation in what follows, the co-ordinate r has been shifted so that the forcing is centred at $r = 0$, rather than at $r = r_f \neq 0$, as was the case for the numerical simulations reported earlier. (In effect, a new variable $\hat{r} = r - r_f$ has been introduced, but it would be rather tedious to keep track of the difference between $\hat{r}$ and r when we turn to making comparisons between the Green's function solutions and the numerical simulation results.)

For the spatially homogeneous case, where U, μ and γ are all taken to be constant, the Green's function solution takes the form

$$G_0(r,t) = \sqrt{\frac{1}{4\pi\gamma t}}\exp\left(\mu t - \frac{(r-Ut)^2}{4\gamma t}\right). \tag{8}$$

It can readily be seen from the above expression that there will be long-term exponential growth at the impulse location $r = 0$, as well as at all other radial locations, whenever

$$\mathfrak{Re}(\mu) > \mathfrak{Re}(U^2/4\gamma). \tag{9}$$

This provides a simple criterion for the onset of absolute instability, which reflects the competition between the effects of linear growth, convection, diffusion and dispersion.

If U and γ are kept constant, but μ is taken to vary linearly according to the relation $\mu = \mu_0 + \mu_1 r$, then Hunt and Crighton showed that the Green's function solution is modified to

$$G(r,t) = \sqrt{\frac{1}{4\pi\gamma t}}\exp\left(\mu t - \frac{(r-Ut)^2}{4\gamma t} + \frac{1}{2}\mu_1 rt + \frac{1}{12}\mu_1^2\gamma t^3\right). \tag{10}$$

It may be seen that the introduction of a linear variation into μ leads to a radical change in the long-term behaviour. This is now dictated by the term $\mu_1^2\gamma t^3$ that appears in the exponential part of the Green's function solution. As Hunt and Crighton pointed out, if μ_1 is purely imaginary and γ has a positive real part (which is usually imposed in order to avoid any negative diffusion), then the disturbance will eventually decay at all locations, no matter how large the linear growth rate $\mathfrak{Re}(\mu) = \mathfrak{Re}(\mu_0+\mu_1 r) = \mathfrak{Re}(\mu_0)$ is taken to be. The local frequency variation, when embodied in an imaginary value for the parameter μ_1, is sufficient to ensure that there is global stability. This can happen, even if there is absolute instability at every spatial point, by which it is meant that the condition stated in Eq. 9 could hold everywhere. (It is perhaps worth remarking that, for configurations where there is marginal absolute stability at all spatial locations, the stabilizing effect of local frequency variation has been familiar to many in the astrophysical fluids-research community for quite some time [17–19]. But awareness of this phenomenon, which has become known as 'phase-mixing', does not seem to have permeated very far, to date, amongst boundary-layer stability researchers.)

Generally, if either of μ_1 or γ is complex, then there will be global stability when

$$\mathfrak{Re}(\mu_1^2\gamma) < 0. \tag{11}$$

If γ is real and positive, then this condition can be satisfied whenever

$$|\mathfrak{Re}(\mu_1)| < |\mathfrak{Im}(\mu_1)|, \tag{12}$$

or in other words, provided that the linear radial variation in the local temporal frequency is stronger than the corresponding variation in the local temporal growth rate. This means that, in particular, there can still be global stability in situations where the local growth rate $\mathfrak{Re}(\mu)$ is continually increasing. For cases where

γ is complex, there is a slightly more complicated balance between the effects of local growth-rate variation and local frequency variation, which is now mediated by an interaction with the effects of diffusion and dispersion. But it remains true that a sufficiently rapid variation in the local frequency will be enough to ensure global stability.

As mentioned previously, Hunt and Crighton obtained Green's function solutions for cases where both U and μ were varied either linearly or quadratically. But in the interest of simplicity, and also because of space limitations, we will not review these solutions in any detail here. Instead we will move on to make some comparisons between the numerical simulation results and the Green's function solution obtained for the one case that we have discussed, namely, where only μ is taken to vary, and it varies in a simple linear manner. Nevertheless, it is perhaps still worthwhile to make a few heuristic remarks to provide a partial justification for limiting our modelling to this single case.

By imposing a linear variation for the local temporal frequency, in conjunction with a linearly increasing local growth rate, we introduce a configuration that, for large enough radii, is much more locally unstable than is actually the case for the rotating-disk boundary layer. This may be seen by referring back to the plots displayed in Fig. 1a, 1c. Recall that these show, respectively, the temporal frequencies and growth rates for the absolute instability that were obtained from a series of numerical simulations for the homogenized flow. The variation of these quantities with the Reynolds number can be expected to dictate the radial dependencies of the local frequency and the local growth rate that must be included in any satisfactory model of the genuine flow that may be constructed using the linearized Ginzburg–Landau equation. The simulation results suggest that, while it is quite reasonable to model the local frequency dependence as being linear in the radius, a better model for the local growth rates could be obtained by taking them to have a quadratic radial variation. But this modification would give only a finite radial interval of absolute instability, which might be anticipated to be somewhat less prone to the generation of global instability than the semi-infinite absolutely unstable region that is entailed when the growth rates are modelled as being linearly increasing.

3.2 Comparisons with numerical simulation results

For the artificial, radially homogenized, version of the rotating-disk flow, it is a fairly straightforward matter to determine constant values of U, μ and γ that give a good fit to the numerical simulation data using a Green's function solution of the form specified in Eq. 8. The constants can all be extracted, in a systematic fashion, from a knowledge of various quantities that can be computed fairly readily from the simulation results. These include the leading- and trailing-edge velocities of the disturbance wavepacket, and the long-term complex frequency, as defined by Eqs. 5 and 6. (The imaginary part of γ, which can be interpreted as representing the effects of dispersion, is perhaps the most difficult constant to deal with. Its determination involves the computation of the radial derivative of a locally defined complex spatial wavenumber.)

Having determined values for U, μ and γ from a radially homogeneous flow simulation conducted at a particular Reynolds number Re, we can then use the same values to specify U, μ_0 and γ, respectively, in the modified Green's function given by Eq. 10. This function, it is presumed, will capture the response of the inhomogeneous flow when it is subjected to an impulsive excitation located at $r_f = \mathrm{Re}$. The only free parameter that remains to be fixed is the complex constant μ_1. This can be found, quite simply, from the radial variation of the locally defined complex frequency. It is easy to show that if $G(r,t)$ is given by Eq. 10, then

$$\frac{\mu_1}{2} = \lim_{t\to\infty} \frac{\partial}{\partial r}\left(\frac{1}{G}\frac{\partial G}{\partial t}\right). \tag{13}$$

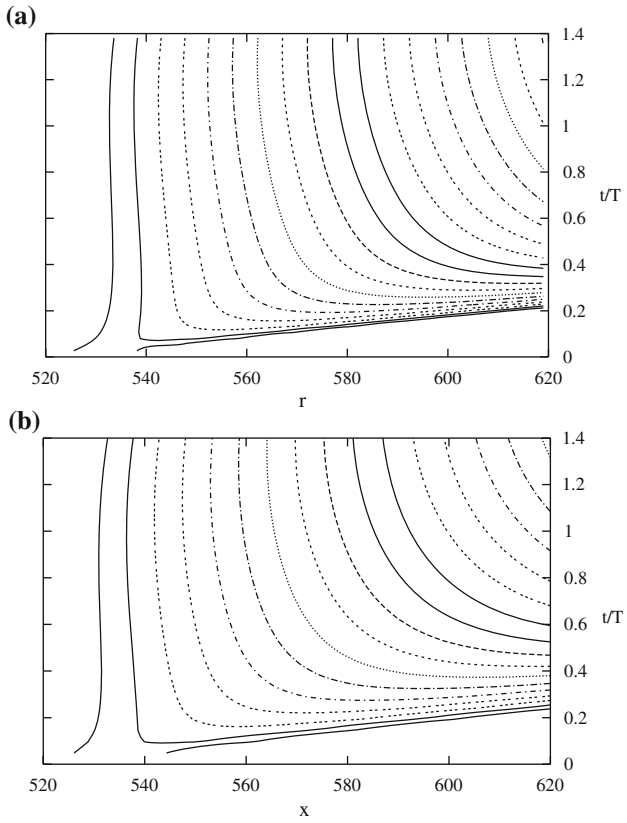

Fig. 5 (**a**) Numerical simulation results for the space–time development of the amplitude modulus $|A(r,t)|$ for an impulsively excited disturbance with $n = 67$ and $r_f = 530$ in the radially inhomogeneous rotating-disk flow. The amplitude is measured by the value of the azimuthal perturbation vorticity at the disk surface. The contours are drawn using a logarithmic scale with a factor of two between successive contours; (**b**) The fitted Green's function solution $|G(x,t)|$ of the form defined in Eq. 10. This represents the impulse response obtained from the linearized complex Ginzburg–Landau equation with a linearly varying complex growth parameter $\mu = \mu_0 + \mu_1(r - r_f)$

This means that if $G(r,t)$ is replaced by the disturbance amplitude $A(r,t)$ obtained from the appropriate inhomogeneous flow simulation, then μ_1 can be computed from the relation

$$\mu_1 = -2\,\mathrm{i}\lim_{t\to\infty}\frac{\partial\tilde{\omega}}{\partial r}, \tag{14}$$

where the locally defined complex frequency $\tilde{\omega}(r,t)$ is specified as in Eq. 5, and a numerical estimate is made for the asymptotic value in the limit.

Figure 5 compares the numerical simulation results for the space–time development of an impulsively excited disturbance in the inhomogeneous flow with the Green's function solution constructed using values of the parameters U, μ_0, μ_1 and γ estimated in the manner that has just been described. It can be seen that there is a good measure of agreement. In particular, the Green's function solution correctly reproduces the behaviour of the trailing edge of the disturbance. Both the numerically simulated disturbance and the Green's function solution display a trailing edge that initially propagates in a radially inward direction, but then reverses direction and starts to propagate radially outwards. Thus there is no sustained temporal growth at the radial position where the impulse is applied.

A more detailed comparison is afforded by considering the evolution of the locally defined complex frequency, as defined by Eq. 5. Simulation results for the real and imaginary parts of the complex frequency were presented in Figs. 3a, 4a, respectively. Both of these figures were discussed in some detail earlier. The corresponding results obtained using the fitted Green's function solution are displayed in Figs. 3b, 4b. It can be seen that there is a very strong similarity between the qualitative form of the behaviour found from the simulations and that which we have derived from our simple model based on the linearized complex Ginzburg–Landau equation. The Green's function correctly predicts the trends of the continually shifting local frequencies, as well as the manner in which the local temporal growth rates decrease and eventually

become negative, leading the disturbance to decay. In fact, there is a surprisingly good level of quantitative agreement, given that the complex quantity μ_1 is the only free parameter that has been introduced in order to capture the differences between the homogenous flow and the genuine radially inhomogeneous flow.

3.3 Global frequency selection

We conclude this modelling section of the paper with a very brief discussion of the global frequency selection criterion that has been developed by Chomaz and others [20–22] for determining the global stability of absolutely unstable flows. The central idea is to deploy a WKBJ type of analysis, made possible by a presumption that there is an underlying slow spatial variation of the basic flow. This slow variation is precisely what is neglected when the parallel-flow approximation is applied, in order to facilitate a locally based linear stability investigation. The WKBJ analysis allows locally derived results to be pieced together, leading to the construction of approximate global modes with a time dependence $\sim \exp(\mathrm{i}\omega_G t)$, whose stability can then be assessed. Limitations of space mean that we will not make any attempt to address or review the subtleties of this process.

The local dispersion relation, as obtained via the use of the parallel-flow approximation, may be cast in terms of the complex temporal frequency ω in the general form

$$\omega = \omega(\alpha, r). \tag{15}$$

In this context, r should be thought of as parameterizing the spatial direction along which the flow is assumed to be slowly varying. It corresponds to the radial direction for the rotating-disk flow, which is reflected in the choice of notation. The complex wavenumber α specifies the normal-mode form of the variation that is prescribed along the same direction, for disturbances evolving in the homogenized version of the basic flow. It can be shown that, subject to the validity of some assumptions about the consequences of the slow spatial development of the basic flow, the complex temporal frequency ω_G for global modes may be fixed by requiring that

$$\frac{\partial \omega}{\partial \alpha} = \frac{\partial \omega}{\partial r} = 0. \tag{16}$$

In other words, a double saddle point is sought. The first of these saddle point requirements is just the usual necessary, but not sufficient, condition that the group velocity must vanish in order for absolutely instability to arise. There is global instability if it is found that the imaginary part of ω_G is positive. But if ω_G has a negative imaginary part, for all eligible saddle points, then the flow is globally stable. A significant feature in the derivation of this result is that, in general, the saddle point obtained with respect to the r variation will be located off from the real axis: the parameter r must be allowed to become complex.

How is the saddle-point result stated above related to the global stability that we have described for the rotating-disk boundary layer? Suppose that the temporal frequency of the absolute instability varies linearly with the radius in the same manner that we have discussed previously, but that the absolute growth-rate varies in a quadratic fashion, giving rise to a finite range of radii over which the flow is absolutely stable. If precisely the same form of variation is assumed to hold for complex values of r, as for the real values, then it is quite straightforward to show that there is a single saddle point in the complex r-plane and to determine its location. It is also a simple matter to verify that the imaginary part of the complex frequency at the saddle point is negative whenever

$$0 < \Im\mathfrak{m}\left(\frac{\mathrm{d}\omega_a}{\mathrm{d}r}\right)_{r=\mathrm{Re}_c} < \left|\Re\mathfrak{e}\left(\frac{\mathrm{d}\omega_a}{\mathrm{d}r}\right)\right|, \tag{17}$$

where $\mathrm{d}\omega_a/\mathrm{d}r$ denotes the rate at which the complex frequency of the absolute instability varies with the radius, with the radius now being kept to be real, and Re_c is the Reynolds number for the onset of absolute instability. $\Re\mathfrak{e}(\mathrm{d}\omega_a/\mathrm{d}r)$ denotes the constant rate at which the absolute temporal frequency increases with

the radius, while $\Im\mathrm{m}(\mathrm{d}\omega_a/\mathrm{d}r)$ is the corresponding, but non-constant, measure of the absolute temporal growth-rate variation. It may be observed that the condition stated in Eq. 17 has the same general form, as a criterion for global stability, as that which was previously stated in Eq. 12. To see this, it should be recalled that μ_1 quantifies the linear radial variation for the complex temporal growth rate, whereas we have now switched our notation in order to consider the radial variation of the complex temporal frequency. Thus the roles of the indicated real and imaginary parts need to be interchanged. But just as before, it can be seen that global stability will be promoted by a sufficiently rapid radial variation in the absolute temporal frequency.

4 Concluding comments

We have examined the global behaviour of linearized disturbances in the von Kármán rotating-disk flow. Our main purpose has been to explain why direct numerical simulations show that the flow remains linearly globally stable, even though it is susceptible to a strong form of absolutely instability.

Analytically specified impulse solutions, derived from a simple linearized amplitude equation, were used to highlight the effects of the radial variation in the temporal frequency of the absolute instability. It was shown that the behaviour of disturbances in the rotating-disk flow could be modelled, in a surprisingly effective manner, by just prescribing a linear relationship between the frequency and the radius. This relationship appears to provide the means for capturing the global stability consequences of a fundamental, but easily overlooked, feature of the rotating-disk flow. Namely, that there is a linear radial increase in the magnitudes of the tangential and radial velocity components of the basic flow, which arises because of the global rotation and the cylindrical geometry.

The impulse solutions that we have considered suggest that, in a more general setting, there will be a competition between the effects of the radial dependence of the absolute temporal frequency and the effects of the corresponding variation in the absolute growth rates. In a related study [23] we found that, by modifying the basic flow through the introduction of mass injection or suction at the disk surface, it is in fact possible to alter the balance so that, in some cases, the variation in the absolute growth rate dominates the variation in the absolute frequency. This leads to an apparently new type of global instability, with the novel feature that, as time passes, there can be increasingly strong temporal growth at a fixed radial position. But there is still no selection of any predominant temporal frequency. Interestingly, this form of instability is promoted by the introduction of mass suction. Previously it had been found that suction has a stabilizing effect on the absolute instability of the rotating-disk flow, at least for the artificially homogenized version of the flow that was considered [6]. The genuine, radially inhomogeneous flow, appears to behave somewhat differently.

Acknowledgements This work was supported in part by the Engineering and Physical Sciences Research Council.

References

1. von Kármán Th (1921)Über laminare und turbulente Reibung. Zeitschrift für angewandte Mathematik und Mechanik 1:233–252
2. Lingwood RJ (1995) Absolute instability of the boundary layer on a rotating-disk. J Fluid Mech 299:17–33
3. Briggs RJ (1964) Electron-Stream Interaction with Plasmas. MIT Press
4. Huerre P, Monkewitz PA (1990) Local and global in stabilities inspatially developing flows. Ann Rev Fluid Mech 22:473-537
5. Huerre P (2000) Open shear flow instabilities. In: Batchelor GK, Moffat HK, Worster MG (eds) Perspectives in fluid Dynamics Springer, pp 159–229
6. Lingwood RJ (1997) On the effects of suction and injection on the absolute instability of the rotating-disk boundary layer. Phys Fluids 9(5):1317–1328

7. Lingwood RJ (1996) An experimental study of absolute instability of the rotating-disc boundary-layer flow. J Fluid Mech 314:373–405
8. Davies C, Carpenter PW (2003) Global behaviour corresponding to the absolute instability of the rotating-disk boundary layer. J Fluid Mech 486:287–329
9. Davies C, Carpenter PW (2001) A novel velocity-vorticity formulation of the Navier–Stokes equations with applications to boundary layer disturbance evolution. J Comp. Phys 172:119–165
10. Othman H, Corke TC (2006) Experimental investigation of absolute instability of a rotating-disk boundary layer. J Fluid Mech 565:63–94
11. Pier B (2003) Finite-amplitude crossflow vortices, secondary instability and transition in the rotating-disk boundary layer. J Fluid Mech 487:315–343
12. Aranson IS, Kramer L (2002) The world of the complex Ginzburg–Landau equation. Rev Modern Phys 74:99–143
13. Gajjar JSB (1996) On the nonlinear evolution of a stationary cross-flow vortex in a fully three-dimensional boundary layer flow. In: Duck PW, Hall P (eds) Nonlinear instability and transition in three-dimensional boundary layers, IUTAM Symposium, Manchester, UK, 1995, Kluwer pp 317–327
14. Gajjar JSB, Arebi MA, Sibanda P (1996) Nonlinear development of cross-flow instabilities in compressible and incompressible boundary layer flows. AIAA Paper No. 96–2159
15. Hunt RE, Crighton DG (1991) Instability of flows in spatially developing media. Proc R Soc London A 435:109–128
16. Hunt RE (1995) Spatially developing flows with localized forcing, PhD Thesis, University of Cambridge
17. Soward AM (1977) On the finite amplitude thermal instability of a rapidly rotating fluid sphere. Geophys Astrophys Fluid Dyn 9:19–74
18. Soward AM (1992) Thin disc kinematic $\alpha\omega$-dynamo models II. Short length scale modes. Geophys Astrophys Fluid Dyn 64: 201–225
19. Harris D Bassom AP, Soward AM (2000) An inhomogeneous Landau equation with application to spherical Couette flow in the narrow gap limit. Physica D 137:260–276
20. Chomaz J-M, Huerre P, Redekopp LG (1991) A frequency selection criterion in spatially developing flows. Studies Appl Math 84:119–144
21. Monkewitz PA, Huerre P, Chomaz J-M (1993) Global linear stability analysis of weakly non-parallel shear flows. J Fluid Mech 251:1–20
22. Cossu C, Chomaz J-M (1997) Global measures of local convective instabilities. Phys Rev Lett 78:4387–4390
23. Davies C, Thomas C (2005) Global stability of the rotating-disk boundary layer and the effects of suction and injection. Bull Am Phys Soc 50(9):266